HSPI The Open Access Publisher

IJPRA ISSN 2766-2748 INTERNATIONAL JOURNAL OF PHYSICS RESEARCH AND APPLICATIONS

Research Article

Determination of the Effect of Zinc Acetate as a Doped Substance on the Properties of Cadmium Sulfide Nanomaterials by using a Hydrothermal Interaction Technique

Mohammed Rasool Ahmed[1], Abdulkareem Thjeel Jabbar[2] and Abdullah Hasan Jabbar[3]*

[1]Jabir ibn Hayyan Medical University, Iraq

[2]Education Directory of Al Muthanaa, Ministry of Education, Iraq

[3]Scientific Research Center, Al-Ayen University, Thi-Qar, Iraq

Abstract

In the current work, cadmium sulfide nanoparticles (CdS) NPs were synthesized via the hydrothermal interaction technique. Especially, the deviation in zinc Acetate $Zn(CH_3CO_2)_2$ with 0.5% 1.5%, and 2.25% was examined for its part in nanoparticles size. The nanoparticle size seems to reduce from 149.7 nm to 116.3 nm by enhancing the zinc acetate $Zn(CH_3CO_2)_2$. With increasing zinc acetate $Zn(CH_3CO_2)_2$ in CdS (Cadmium Sulfide) small lattice phase changes appeared due to angle peaks of diffraction shifting toward higher angle. The standard crystallite size and lattice parameters were analyzed through X-ray diffraction (XRD) characterization. The average crystallite size and volume unit cell were found to increment with increasing Zinc acetate $Zn(CH_3CO_2)_2$ concentrations. Absorption peaks in the UV visible spectra corresponding to zinc acetate $Zn(CH_3CO_2)_2$ of CdS (Cadmium Sulfide) were analyzed at various wavelengths of 368 nm and 369 and 371nm. These findings show the tuning ability of structural, and optical characteristics of cadmium sulfide (CdS) NPs.

More Information

***Address for correspondence:** Abdullah Hasan Jabbar, Scientific Research Center, Al-Ayen University, Thi-Qar, Iraq, Email: physics1984@yahoo.com; abdullah.hasan@alayen.edu.iq

Submitted: September 05, 2023
Approved: September 13, 2023
Published: September 14, 2023

How to cite this article: Ahmed MR, Jabbar AT, Jabbar AH. Determination of the Effect of Zinc Acetate as a Doped Substance on the Properties of Cadmium Sulfide Nanomaterials by using a Hydrothermal Interaction Technique. Int J Phys Res Appl. 2023; 6: 160-164.

DOI: 10.29328/journal.ijpra.1001066

Keywords: Structural; Morphological; CdS; $Zn(CH_3CO_2)_2$

Abbreviations: NPs: Nanoparticles; XRD: X-Ray Diffraction; FWHM: Full Width at Half Maximum; SEM: Scanning Electron Microscopy; FSEM: Field Scanning Electron Microscopy; FESEM: Field Emission Scanning Electron Microscopy; CdS: Cadmium Sulfide; $Zn(CH_3CO_2)_2$: Zinc Acetate Formula; UV: Ultra Violate

Introduction

Nobel nanoparticles NPs due to noticeable uses in numerous areas such as optics, catalysis, and anti-bacterial are currently taking the moral consideration of researchers. Nobel NPs get effective competencies when their photovoltaic and optoelectronic properties are altered by modifying their size, composition, density, fabrication route, and particle shape [1].

Cadmium sulfide (CdS) NPs is extremely utilized owing to energy storage devices, solar cell, photoconductor, photo-detectors, and photovoltaic device applications. These nanoparticles have a major role in photovoltaic as well as electronic storage devices. Because of its appropriate and significant bandgap, CdS nanoparticles are also utilized in photovoltaic, UV detectors, radar systems, the food industry, and diagnostic [2].

Nanotechnology concerns the growth of fast and dependable experimental procedures for nanomaterials synthesis over chemical composition, industrial scale, and particle size. Nano-materials can be fabricated via numerous techniques, such as chemical and green techniques [3]. The chemical fabrication techniques need a shorter interval for fabricating the large amount of nanoparticles [4,5].

Cadmium sulfide (CdS) NPs can be prepared via numerous fabrication techniques, such as chemical and photochemical reactions in reduction reaction in solutions thermal decomposition of CdS compounds, reverse micelles, electrochemical, newly synthesized by hydrothermal and radiation assisted techniques [6,7]. It is easily scaled up, environmentally friendly for large manufacturers, and inexpensive. The best advantage of this material is homogeneity can be obtained which proves best for the properties of the synthesized material. The only disadvantage of hydrothermal is that synthesized material is obtained in small quantities. In the current method, there is no need to utilize higher

temperatures, pressure, energy, and toxic chemicals. Out of several techniques, one is a wet chemical preparation route which gives the best potential for the worthwhile and large-scale preparation of Cadmium sulfide (CdS) NPs [8-10].

Hydrothermal interaction is a prominent method that is utilized in current work for the preparation of cadmium sulfide NPs. Hydrothermal interaction is an appropriate technique for the synthesis of CdS NPs. Hydrothermal interaction is a fast inexpensive method that can be adjusted at modest room temperature, minimum gas flow rate, modest pressure, suitable current, and voltage. The key problem is this combination of nanoparticles after the synthesis. Consequently, nonuniformity and non-homogeneity and we described for the first time in the production of CdS NPs.

Methodology

Cadmium Sulfide (CdS) NPs through the hydrothermal method. (0.25g) of cadmium acetate $(CH_3.COO)_2Cd.\ 2H_2O$ and (0.75 g) of Thiourea $NH_2.CS.NH_2$ dissolved in 50 ml of deionized water with a ratio of (1:3) as a sample1. Then (0.5%, 1.5%, and 2.25%) of Zinc acetate $Zn(CH_3CO_2)_2$ are mixed in samples respectively. The solution was assorted through a magnetic stirrer by continuously stirring for 10 min. Then 50 ml of the produced solution was added into the Teflon-lined stainless-steel autoclave and heated in an oven at reaction temperature 170 °C for 3 h, and cold down at room temperature. The centrifuge (Frontier 5706) was used to separate the obtained solution at 5000 rpm for 10 min to obtain the deep-yellow powder. The resultant sample (CdS) was washed two or three times through absolute ethanol (C_2H_5OH) purity (99.9%) and deionized water and then dried at 70 °C (Figure 1).

X-ray diffraction (XRD) and Scanning Electron Microscopy (SEM) were utilized for the structural and morphological analysis of cadmium sulfide NPs.

Results and discussions

XRD analysis

The XRD graph of CdS NPs is shown in Figure 2 revealing the amorphous and crystalline phases. The crystalline peaks show the face-centered cubic (FCC) structure of CdS nanomaterials [11-14]. All specimens exhibited the FCC structure which was revealed from the XRD graph as exhibited as shown in Figure 2. Lattice parameters, crystallite size, and some other structural features were observed from XRD-examined data of CdS NPs. Debye-Scherrer equation was used to calculate the crystallite size of NPs [15].

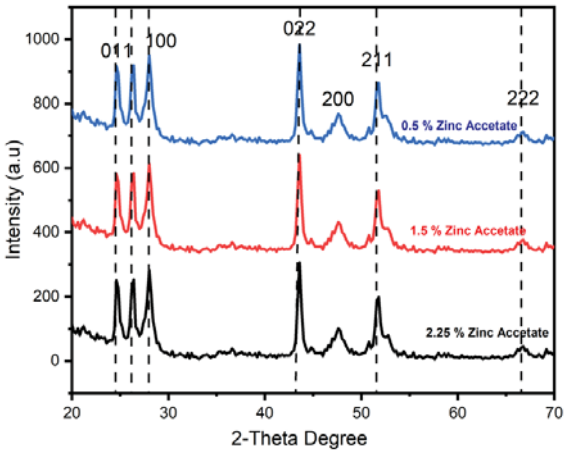

Figure 2: XRD peaks of CdS NPs prepared through different concentrations of zinc acetate (0.5%, 1.5%, and 2.5%).

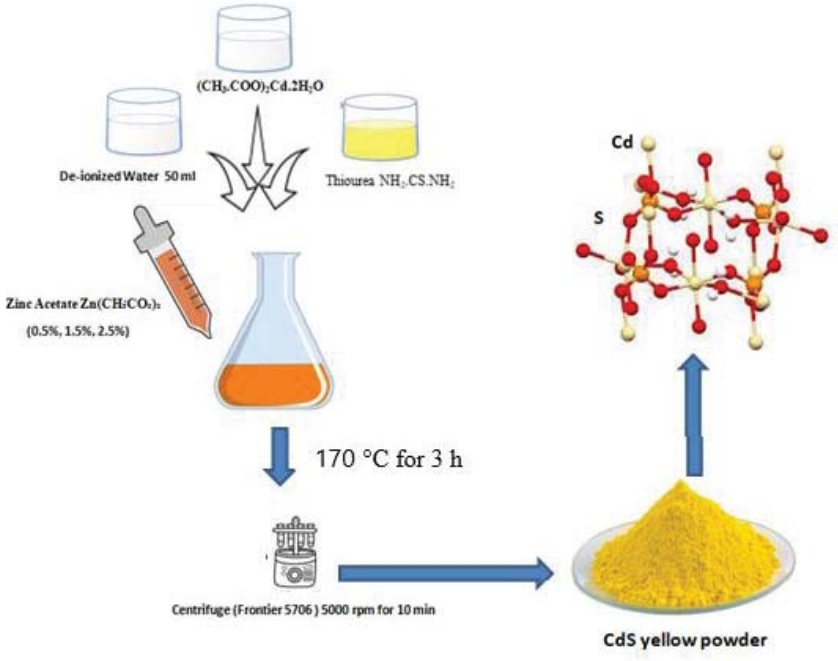

Figure 1: Experimental diagram of sample preparation of CdS at different concentrations of zinc acetate (0.5%, 1.5%, and 2.5%)

$$D = \frac{K\lambda}{\beta Cos\Theta} \quad (1)$$

Where β represents the full width at half maximum (FWHM) of the XRD peak, λ is the X-ray wavelength and θ is the Bragg diffraction angle. In the current work, Scherrer's formula was used to determine the size of crystallite for all specimens which were 7.87 nm, 7.63 nm and 5.89 nm for the specimens synthesized through zinc acetate (0.5%, 1.5% and 2.5%) respectively as shown in Table 1. The examined crystallite size lies in the favorite nanometer range; consequently, these synthesized CdS NPs are appropriate for photovoltaic applications.

Bragg's law formula was used to determine the d-spacing was equivalent to (111) distinguishing peak which is given below [16,17].

$$d = \frac{\lambda}{2\sin\theta} \quad (2)$$

The d-spacing was 4.26355Å, 3.8564Å, and 3.8628Å of the specimens prepared through zinc acetate (0.5%, 1.5% and 2.5%) respectively. The d-spacing declined with the reduction in crystalline size which is given in Table 1.

The following formula was used to measure the lattice constant of cubic phase CdS [18]:

$$a = d\sqrt{h^2 + l^2 + k^2} \quad (3)$$

The unit cell constant declined from 4.26355Å to 3.8628Å.

The following formula was used to estimate the unit cell volume of CdS [19].

$$V_{cell} = a^3 \quad (4)$$

The following formula was applied to determine the X-ray density (ρ_{XRD}) of the CdS [20].

$$\rho_{XRD} = \frac{8M}{Na^3} \quad (5)$$

The X-ray density was enhanced from 1.85% to 9.22%.

The equation was used to determine the bulk density (ρ_B) of the CdS is given below [21].

$$\rho_B = \frac{m}{V} \quad (6)$$

Where m and v are the mass of each sample and lattice volume of each unit cell, respectively. The calculated values were improved from 1.72 g/cm^3 to 8.68 g/cm^3.

The following relation of bulk density and X-ray density was used to estimate the porosity of the samples [22].

$$\text{Porosity} = \left(1 - \frac{\rho B}{\rho x}\right) \times 100\% \quad (7)$$

The porosity was reduced from 8.03% to 5.92%. 0.5%. The results exhibited that the porosity exhibited the reverse behavior to the bulk density with the change in material.

Dislocation density

The formula used to determine the dislocation density in the samples is given below [23-25].

$$\delta_{hkl} = 1/D^2 \quad (8)$$

Where "D" is the crystallite size determined using Sherrer's formula. With the increase in concentration, dislocation density was increased which belongs to the crystallite size. With the increase in crystallite size, the dislocation density was increased. With higher concentrations, nanoparticles show higher irregularity in the crystals. The results are presented in Table 2.

Morphology

In the micrograph, the Cds NPs are visible at greater magnification (100,000x). To investigate the morphological characteristics of CdS NPs, a Field Scanning Electron Microscopy (FSEM) examination was done. The size of the particles was estimated using FSEM analysis and is shown in Figure 3's micrographs. FSEM made use of FSEM grids that were made using specimen powder on a grid coated in copper. A light was used to dry the grid Grain boundaries in specimen 1 were not distinct, the specimen showed more agglomeration, and the specimen showed 8.03% porosity, as revealed by XRD data. In specimen 2, the specimen exhibited the reduced agglomeration that specimen 1, and the specimen exhibited a porosity of 6.56%. In specimen 3, grain boundaries were uniformly distributed and clear. The sample showed no agglomeration while the specimen exhibited 5.92% porosity. The particle size appears to decrease from 149.7 nm to 116.3 nm by increasing the of zinc acetate $Zn(CH_3CO_2)_2$ with 0.5% 1.5% and 2.25%. In all samples, agglomeration was highly increased. The increasing agglomeration becomes a cause for the reduction in particle size. The reason is that the higher magneticity among grains becomes a cause behind the increase in agglomeration. The increasing agglomeration

Table 2: The values of dislocation densities of zinc acetate (0.5%, 1.5%, and 2.5%) of zinc acetate are given below.

Samples	Density Dislocation
0.5%	0.016145
1.5%	0.017177
2.25%	0.028825

Table 1: Different parameters to study the zinc acetate (0.5%, 1.5% and 2.5%) of zinc acetate.

Crystallite Size (nm)	d-spacing (Á)	Dislocation Density	Lattice Constant	Lattice Volume	X-ray Density (g/cm^3)	Bulk Density (g/cm^3)	Porosity (%)
7.78	2.3467	0.017156	4.3642	78.1532	1.7483	1.68	8.13
7.53	2.2789	0.015169	3.8561	61.5361	2.3022	2.25	6.45
5.98	2.2569	0.02775	3.8528	15.5425	9.2314	7.67	5.89

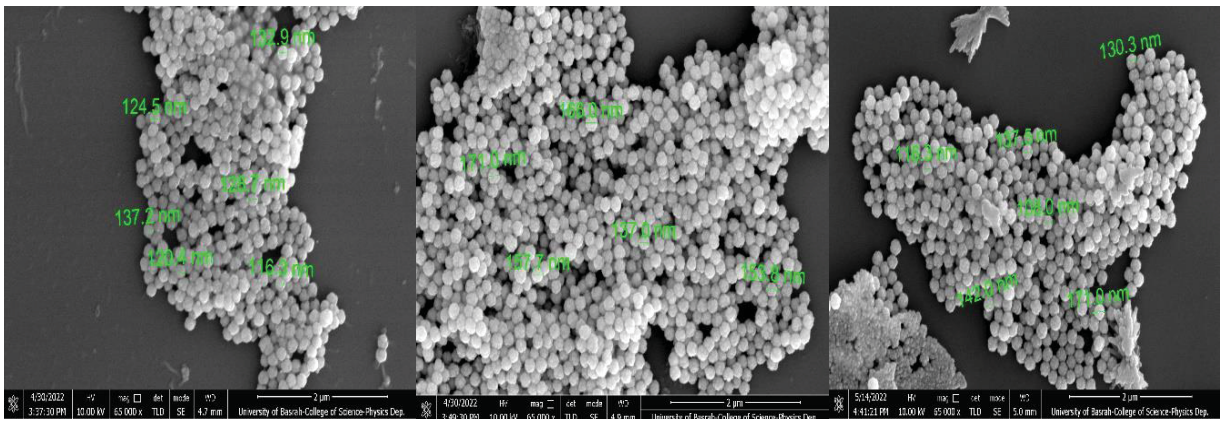

Figure 3: Field Emission Scanning Electron Microscopy (FESEM) micrographs of CdS nanoparticles synthesized by various zinc acetate (0.5%, 1.5% and 2.5%).

becomes a cause behind the reduction in particle size. The reason is that due to increasing agglomeration, the particles cannot grow because of the high forces of attraction among the nanoparticles. Therefore, particles cannot grow with the increase in agglomeration.

Conclusion

In the current work, CdS NPs were synthesized by the hydrothermal technique. Particularly, the change in zinc Acetate $Zn(CH_3CO_2)_2$ with the concentration of 0.5% 1.5% and 2.25% was examined for its role in nanoparticles size. The particle size seems to reduce from 149.7 nm to 116.3 nm by enhancing the zinc acetate $Zn(CH_3CO_2)_2$ with the mentioned concentrations. With increasing zinc acetate $Zn(CH_3CO_2)_2$ in CdS (Cadmium Sulfide) small lattice phase changes appeared due to angle peaks of diffraction shifting toward higher 2θ for samples. The average crystallite size and lattice constant were analyzed through XRD characterization. The average crystallite size and volume unit cell were found to increment with increasing zinc acetate $Zn(CH_3CO_2)_2$ concentrations. These findings show the tuning ability of structural characteristics of cadmium sulfide (CdS) NPs.

References

1. Salavati-Niasari M, Esmaeili E, Davar F. Synthesis and characterization of cadmium sulfide nanostructures by novel precursor via hydrothermal method. Comb Chem High Throughput Screen. 2013 Jan;16(1):47-56. doi: 10.2174/1386207311316010007. PMID: 23190555.

2. Kuang PY, Zheng PX, Liu ZQ, Lei JL, Wu H, Li N, Ma TY. Embedding Au Quantum Dots in Rimous Cadmium Sulfide Nanospheres for Enhanced Photocatalytic Hydrogen Evolution. Small. 2016 Dec;12(48): 6735-6744. doi: 10.1002/smll.201602870. Epub 2016 Oct 6. PMID: 27709776.

3. Jameel MH, Saleem S, Hashim M, Roslan MS, Somaily HHN, Hessein MM, El-Bahy ZE, Ashiq MGB, Hamza MQ. A comparative study on characterizations and synthesis of pure lead sulfide (PbS) and Ag-doped PbS for photovoltaic applications. Nanotechnology Reviews. 2021; 10(1): 1484-1492.

4. Vu TTD, Mighri F, Ajji A, Do TO. Synthesis of titanium dioxide/cadmium sulfide nanosphere particles for photocatalyst applications. Industrial & Engineering Chemistry Research. 2014; 53(10): 3888-3897.

5. Hassan M, Gondal MA, Cevik E, Dastageer MA, Baig U, Moqbel RA, Al Abass N. Laser-assisted anchoring of cadmium sulfide nanospheres into tungsten oxide nanosheets for enhanced photocatalytic and electrochemical energy storage applications. Colloids and Surfaces A: Physicochemical and Engineering Aspects. 2021; 617: 126318.

6. Ma X, Zhu Y, Lu L, Liang C, Chen Q Liao Y. Particle Size and Temperature Effects on Surface Thermodynamic Functions and Particle Size Effects on Prescribed Thermodynamic Functions for Cadmium Sulfide Nanospheres. Materials Chemistry and Physics. 2021; 260: 124050.

7. Tan P, Zhu A, Qiao L, Zeng W, Cui H, Pan J. Manganese oxide at cadmium sulfide (MnOx@CdS) shells encapsulated with graphene: A spatially separated photocatalytic system towards superior hydrogen evolution. J Colloid Interface Sci. 2019 Jan 1;533:452-462. doi: 10.1016/j.jcis.2018.08.102. Epub 2018 Aug 29. PMID: 30172771.

8. Leal-Cruz AL, Berman-Mendoza D, Vera-Marquina A, García-Juárez A, VillaVelazquez-Mendoza C, Zaldívar-Huerta IE. Synthesis and characterization of CBD-CdS nanospheres. In CONIELECOMP 2013, 23rd International Conference on Electronics, Communications, and Computing. IEEE. 2013; 260-263.

9. Gupta N, Pal B. The synthesis, structure, optical and photocatalytic properties of silica-coated cadmium sulfide nanocomposites of different shapes. J Colloid Interface Sci. 2012 Feb 15;368(1):250-6. doi: 10.1016/j.jcis.2011.11.022. Epub 2011 Nov 25. PMID: 22154910.

10. Wei C, Zang W, Yin J, Lu Q, Chen Q, Liu R, Gao F. Biomolecule-assisted construction of cadmium sulfide hollow spheres with structure-dependent photocatalytic activity. Chemphyschem. 2013 Feb 25;14(3):591-6. doi: 10.1002/cphc.201200862. Epub 2013 Jan 7. PMID: 23297031.

11. Ganesh RS, Sharma SK, Durgadevi E, Navaneethan M, Binitha HS, Ponnusamy S, Kim DY. Surfactant-free synthesis of CdS nanospheres, microstructural analysis, chemical bonding, optical properties, and photocatalytic activities. Superlattices and Microstructures. 2017; 104: 247-257.

12. Shvalagin VV, Stroyuk AL, Kotenko IE, Kuchmii SY. Photocatalytic formation of porous CdS/ZnO nanospheres and CdS nanotubes. Theoretical and Experimental Chemistry. 2017; 43(4): 229-234.

13. Saleem S, Jameel MH, Akhtar N, Nazir N, Ali A, Zaman A, Althubeiti K. Modification in structural, optical, morphological, and electrical properties of zinc oxide (ZnO) nanoparticles (NPs) by metal (Ni, Co) dopants for electronic device applications. Arabian Journal of Chemistry. 2022; 15(1): 103518.

14. Saleem S, Jameel MH, Rehman A, Tahir MB, Irshad MI, Jiang ZY, Hessien MM. Evaluation of Structural, Morphological, Optical, and Electrical Properties of Zinc Oxide Semiconductor Nanoparticles with

Microwave Plasma Treatment for electronic device Applications. Journal of Materials Research and Technology. 2022; 19: 2126-2134.

15. Jameel MH, Ahmed S, Jiang ZY, Tahir MB, Akhtar MH, Saleem S, Roslan MS. First principal calculations to investigate structural, electronic, optical, and magnetic properties of Fe3O4 and Cd-doped Fe2O4. Computational Condensed Matter. 2022; 30: e00629.
16. Wang Y, Wang Y, Xu R. Synthesis of Zn–Cu–Cd sulfide nanospheres with controlled copper locations and their effects on photocatalytic activities for H2 production. International journal of hydrogen energy. 2010; 35(11): 5245-5253.
17. Wu Y, Wang H, Tu W, Wu S, Chew JW. Construction of hole-transported MoO3-x coupled with CdS nanospheres for boosting photocatalytic performance via oxygen-defects-mediated Z-scheme charge transfer. Applied Organometallic Chemistry. 2019; 33(4): e4780.
18. Zang Y, Cao R, Zhang C, Xu Q, Yang Z, Xue H, Shen Y. TiO2-sensitized double-shell ZnCdS hollow nanospheres for photoelectrochemical immunoassay of carcinoembryonic antigen coupled with hybridization chain reaction-dependent Cu2+ quenching. Biosens Bioelectron. 2021 Aug 1;185:113251. doi: 10.1016/j.bios.2021.113251. Epub 2021 Apr 17. PMID: 33905965.
19. Abdullah U, Ali M, Pervaiz E. An inclusive review on recent advancements of cadmium sulfide nanostructures and its hybrids for photocatalytic and electrocatalytic applications. Molecular Catalysis. 2021; 508: 111575.
20. Mezan SO, Al Absi SM, Jabbar AH. Synthesis and characterization of enhanced silica nanoparticle (SiO2) prepared from rice husk ash immobilized of 3-(chloropropyl) triethoxysilanea. Materials Today: Proceedings. https://doi.org/10.1016/j.matpr.2020.12.564
21. Turki Jalil A, Hussain Dilfy S, Oudah Meza S, Aravindhan S, Kadhim MM, Aljeboree MA. CuO/ZrO2 Nanocomposites: Facile Synthesis, Characterization and Photocatalytic Degradation of Tetracycline Antibiotic. Journal of Nanostructures. 2021; 11(2): 333-341. DOI: 10.22052/JNS.2021.02.014
22. Maseer MM, Alnaimi FBI, Hannun RM, Wai LC, Al-Gburi KAH, Mezan SO. A review of the characters of nanofluids used in the cooling of a photovoltaic-thermal collector, Materials Today: Proceedings. https://doi.org/10.1016/j.matpr.2021.09.214
23. Al Absi SM, Jabbar AH, Oudah Mezan S. An experimental test of the performance enhancement of a Savonius turbine by modifying the inner surface of a blade. Materials Today: Proceedings. https://doi.org/10.1016/j.matpr.2020.12.309
24. Altajer AH, Amri Tanjung F, Hasan Jabbar A, Oudah Mezan S, Thangavelu L, Kadhim MM, Alkaim AF. Novel Carbon Quantum Dots: Green and Facile Synthesis, Characterization and its Application in On-off-on Fluorescent Probes for Ascorbic Acid. J Nanostruct. 2021; 11(2): 236-242. DOI: 10.22052/JNS.2021.02.004.
25. Mezan SO. Silica/Polystyrene Nanocomposite (SiO2/PsNCs) using Sol-Gel Method Drug Delivery System: A Review. Design Engineering. 2021; 10175-10181.